Acta Pharm. **67** (2017) 557–567

Original research paper

https://doi.org/10.1515/acph-2017-0032

A study on blocking store-operated Ca^{2+} entry in pulmonary arterial smooth muscle cells with xyloketals from marine fungi

JIE-BIN ZHOU[1,a]
YING-YING SUN[2,a]
YING-LIN ZHENG[1]
CHU-QIN YU[2]
HUA-QING LIN[2,*]
JI-YAN PANG[1,*]

[1] *School of Chemistry Sun Yat-Sen University, Guangzhou 510275, P. R. China*

[2] *Department of Guangdong Key Laboratory for New Pharmaceutical Dosage Forms GuangDong Pharmaceutical University, Guangzhou 510006, P. R. China*

Accepted June 22, 2017
Published online August 25, 2017

In this study, the effect of four xyloketals **1**-**4** on store-operated calcium entry (SOCE) was investigated in primary distal pulmonary arterial smooth muscle cells (PASMCs) isolated from mice. The results showed that xyloketal A (**1**), an unusual ketal with C-3 symmetry, exhibited strong SOCE blocking activity. Secretion of interleukin-8 (IL-8) was also inhibited by xyloketal A. The parallel artificial membrane permeability assay (PAMPA) of **1**-**4** suggested that these xyloketals penetrated easily through the cell membrane. Moreover, the molecular docking study of xyloketal A with activation region of the stromal interaction molecule (STIM) 1 and the calcium release-activated calcium modulator (ORAI) 1 (STIM1-ORAI1) protein complex, the key domain of SOCE, revealed that xyloketal A exhibited a non-covalent interaction with the key residue lysine 363 (LYS363) in the identified cytosolic regions in STIM1-C. These findings provided useful information about xyloketal A as a SOCE inhibitor for further evaluation.

Keywords: xyloketal A, store-operated calcium entry, molecular docking, IL-8, parallel artificial membrane permeability assay

Store-operated calcium entry (SOCE) is the central mechanism in cellular calcium signaling and in maintaining cellular calcium balance. It plays an important role in regulating calcium signaling and cellular responses in different cell types, such as airway smooth muscle cells (ASMCs) (1), polarized cells (2), endothelial cells (3), and pulmonary arterial smooth muscle cells (PASMCs) (4, 5). Along this line, SOCE deregulation is involved in the development of various diseases, such as hypertension (6, 7), stroke (8, 9), diabetes (10), cancer (11–14), pulmonary arterial hypertension (PAH) (15), and others (16, 17). Experiments have revealed the essential role of stromal interaction molecule (STIM) 1 as calcium sensor at the endoplasmic reticulum and plasma membrane calcium release-

[a] These authors contributed equally to this work.

* Correspondence; e-mails: cespjy@mail.sysu.edu.cn; huaqing_@vip.tom.com

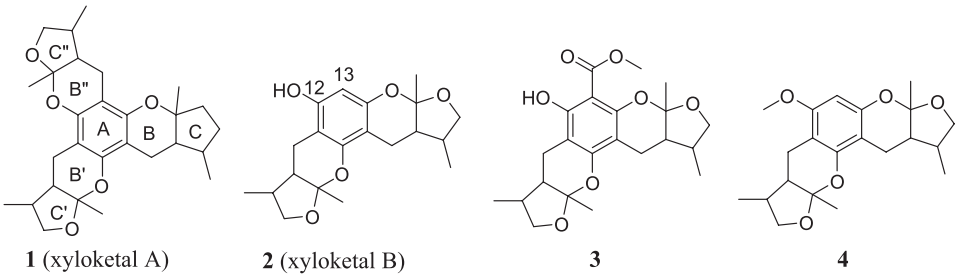

1 (xyloketal A) **2** (xyloketal B) **3** **4**

Fig. 1. Structures of xyloketal A (**1**), xyloketal B (**2**) and two xyloketal derivatives **3** and **4**.

activated calcium channel protein 1 (named ORAI1) in mediating SOCE because these proteins sense and respond to endoplasmic reticulum calcium store depletion (18).

PAH is a rare life-threatening disease, and although significant progress has been made in the past decades in our understanding of PAH pathophysiology and treatment, the prognosis is still poor. It was previously demonstrated in PASMC that influx of Ca^{2+} through transient receptor potential (TRP) proteins is likely to play a significant role in the development of chronic hypoxic PAH (15). In line with recent discoveries of the STIM1-ORAI1 role in SOCE, it seems that these proteins may serve as important targets for PAH treatment.

Marine environment is a rich source of novel compounds and unusual secondary metabolites, many of which show promise as therapeutic agents. Xyloketals, a type of novel compounds possessing unique molecular structures, were isolated from the marine mangrove fungus *Xylaria* sp. (19, 20). In particular, xyloketal A is a unique ketal compound with C-3 symmetry with *cis*-junction between tetrahydropyrane and tetrahydrofurane. We have previously demonstrated that xyloketals show a variety of activities, such as antioxidant (21), promoting endothelial cell nitric oxide (NO) production, inhibiting NADPH oxidase, and L-calcium channel blocking in different disease models (22–24). Xyloketals have been previously reported to inhibit Ca^{2+} influx through blockade of L-type calcium channels, which raises the possibility that xyloketals might affect calcium signaling in diseases like chronic hypoxic pulmonary hypertension. We have therefore investigated the potential of a series of xyloketals: xyloketal A (**1**), xyloketal B (**2**), and other two xyloketal derivatives (**3** and **4**) (Fig. 1) on SOCE in primary distal pulmonary arterial smooth muscle cells (PASMCs) isolated from mice. In addition, their effect on secretion of interleukin-8 (IL-8), an important pro-inflammatory chemokine in airway epithelia, was tested. A parallel artificial membrane permeability assay (PAMPA) of these xyloketals was carried out to explore their permeability. Further, a molecular docking study of a selected compound with STIM-ORAI activating region (SOAR) was performed to characterize their interactions.

EXPERIMENTAL

Reagents

Dulbecco's modified Eagle's medium (DMEM) and fetal bovine serum (FBS) were purchased from Gibco, USA. All other reagents utilized were purchased from Sigma

Chemical Co. USA, unless otherwise specified. Xyloketals **1**-**4** were obtained from the School of Chemistry, Sun Yat-Sen University, Guangzhou, China. Identity and purity of the compounds were determined using HPLC (high performance liquid chromatography) and NMR, as previously described (19, 23), and were > 95 %. Xyloketals were dissolved in dimethyl sulfoxide (DMSO) and stored at –20 °C until use. Final concentration of DMSO in the culture media was ≤ 0.1 %.

PASMCs cells' isolation and culture

Distal intrapulmonary arteries and intrapulmonary veins were dissected from the lungs of adult male C57BL/6 mice (20–25 g) purchased from the Guangdong Medical Laboratory Animal Center (Guangzhou, Guandong, China). All animal experiments were approved by the Animal Care and Use Committee of Sun Yat-sen University, and all animal care and experimental procedures strictly followed the Council for International Organizations of Medical Sciences (CIOMS) guidelines. Primary cultures of PASMCs were prepared from the lungs of animals. Briefly, animals were humanely killed by cervical dislocation. Distal (> 4th generation) intrapulmonary arteries were dissected from the lungs. A thin layer of adventitia was carefully stripped off with fine forceps, and the endothelium was wiped off using a cotton swab. Lumina were gently swiped using a cotton swab to remove endothelium. Distal PASMCs were obtained from the isolated pulmonary arteries (PA) by enzymatic dissociation (papain and collagenase IA, Sigma-Aldrich, USA) in medium according to the described protocol (25, 26). Purity was > 98 %, which was checked by the morphological appearance under phase-contrast microscopy (IX73, Olympus, Japan). Isolated cells were then seeded in 6-well culture dishes and cultured in smooth muscle growth medium-2 (Clonetics, USA) in a humidified atmosphere of 5 % CO_2 and 95 % air at 37 ºC for 3 to 4 days. PASMCs were replaced with smooth muscle basal medium (Clonetics) containing 0.3 % FBS for 24 h to reach growth arrest for the treatment of substances. Before measuring the intracellular Ca^{2+} concentration, PASMCs were treated with compounds **1**-**4** (5 mmol L^{-1}) for 4–6 h.

Measurement of intracellular Ca^{2+}

Intracellular Ca^{2+} concentration was measured according to the reported protocol (27, 28). Coverslips with PASMCs were incubated with 5 μmol L^{-1} calcium indicator fura-2 acetoxymethyl ester (Invitrogen, USA) for 60 min at 37 °C with 5 % CO_2-95 % air, mounted in a closed polycarbonate chamber and clamped to a heated aluminum platform (PH-2, Warner Instrument, USA) on the stage of a Nikon TSE 100 Ellipse inverted microscope (Nikon, USA). The chamber was perfused with Krebs Ringer bicarbonate (KRB) solution equilibrated with 16 % O_2 and 5 % CO_2 at 38 °C at 0.5–1 mL min^{-1} in heated reservoirs. Perfusate was led *via* stainless steel tubing and a manifold to an inline heat exchanger (SF-28, Warner Instrument) to rewarm the perfusate just before it entered the cell chamber. Temperature of the heat exchanger and chamber platform was controlled by a dual-channel heater controller (TC-344B, Warner Instrument). To remove the extracellular dye and to allow the intracellular esterases to cleave cytosolic fura-2-AM into active fura-2, the cells were perfused with modified Krebs solution for 10–15 min. Fura-2 fluorescence was observed as a 510-nm light emission with excitation wavelengths of 340 and 380 nm. Intracellular Ca^{2+} concentration ($[Ca^{2+}]_i$) was determined at 12- to 30-s intervals from the ratio of

fura-2 fluorescence after excitation at 340 nm to that after excitation at 380 nm (F_{340}/F_{380}) in 20–30 cells using a fluorescence imaging system that consisted of a xenon arc lamp, interference filters, an electronic shutter, a 20× fluorescence objective and a cooled charge-coupled device imaging camera. Data were collected using InCyte software (Intracellular Imaging Inc, USA). In all experiments, multiple cells were imaged in a single field and one randomly chosen peripheral cytosolic area from each cell was averaged. Resting $[Ca^{2+}]_i$ was obtained by average F_{340}/F_{380} during the initial modified Krebs solution (MKS) recording. Changes in $[Ca^{2+}]_i$ were calculated as peak F_{340}/F_{380} minus the averaged steady-state F_{340}/F_{380} in the 20 s preceding the rise to a peak. All time periods under each condition were kept constant during the experiments (27).

Assessment of SOCE

We assessed SOCE after Ca^{2+} restoration according to the described protocol (27, 28). Briefly, PASMCs were perfused for 10-15 min with Ca^{2+}-free KRB solution containing 5 mmol L^{-1} nifedipine, 10 mmol L^{-1} cyclopiazonic acid (CPA), and 1 mmol L^{-1} ethylenediaminetetraacetic acid (EDTA). We first measured $[Ca^{2+}]_i$ at 0–5 min intervals before and after restoration of extracellular $[Ca^{2+}]$ to 2.5 mmol L^{-1}. SOCE was evaluated from the increase in $[Ca^{2+}]_i$ caused by restoration of extracellular $[Ca^{2+}]_i$.

Preparation of cigarette smoke extraction (CSE) and cell stimulation

CSE was prepared by bubbling smoke from 2 cigarettes (purchased from Guangzhou, China, with ~0.8 mg nicotine per cigarette) into 10 mL of serum-free DMEM and then CSE was sterile-filtered through a 0.2-mm filter (VWR International, USA). This medium was defined as 100 % CSE while with the concentration of 1 % CSE cell inflammation was induced. Human bronchial epithelial cells Beas-2b and 16 HBE (purchased from ATCC, Manassas, VA, USA) were grown in high-glucose DMEM medium, with 10 % fetal bovine serum, 100 U mL^{-1} penicillin and 0.1 mg mL^{-1} streptomycin. Cells were first treated with xyloketal A 5 mmol L^{-1} for 2 h, and then 1 or 2 % CSE was added for 24 h.

Enzyme-linked immunosorbent assay (ELISA) for IL-8 detection

Cultured media were collected at the end of experimental procedures. Levels of IL-8 secreted from cultured cells were quantified using the IL-8 Elisa kit (BD Biosciences, USA) according to the manufacturer's protocol.

Parallel artificial membrane permeability assay (PAMPA)

In PAMPA, a „sandwich" structure was formed by a 96-well microtiter plate and a 96-well filter plate, coated with dried 15 μL of 10 % *m*/*V* lecithin/dodecane (Egg-PAMPA) or 5 % *m*/*V* hexadecane/dodecane (HDM-PAMPA) according to the protocol described in ref. 29. Solutions of xyloketals **1**-**4** together with the positive controls verapamil, atenolol and ciprofloxacin were added to the wells (100 μL per well) on a pre-coated filter, and phosphate buffer saline (pH 7.4) was added to the wells (375 μL per well) on the receiver plate. Filter plate was coupled with the receiver plate and the sandwich was incubated in the thermostat at 37 °C for 16 h or 5 h under shaking at 80 rpm. After incubation, the plates

were separated and sample solutions from each well of both the filter plate and the receiver plate were transferred to tubes. Samples were analyzed by HPLC (30) and permeability was calculated:

$$\log P_e = \log \frac{V_D V_A}{V_D V_A A t} \ln \frac{[\text{drug}]_{eq}}{[\text{drug}]_{acc}}$$

where V_D is the donor compartment volume, V_A is the acceptor compartment volume, A is the effective area of the membrane insert and t is time. Here, A is 0.28 cm^2, $[drug]_{acc}$ refers to the concentration of the tested drug in the acceptor compartment, $[drug]_{eq}$ is the concentration of the tested drug in the equilibrium mixture, and time is the total transport time in seconds. Technical specification is in Egg-PAMPA, membrane permeability $\log P_e > -5.0$ is easily permeable, $-5.0 > \log P_e > -6.0$ is moderately permeable, and $\log P_e < -6.0$ is hardly permeable. In HDM-PAMPA, membrane permeability of $\log P_e > -4.0$ is easily permeable; $-4.0 > \log P_e > -5.0$ is moderately permeable, and $\log P_e < -5.0$ is hardly permeable.

The HPLC (LC-2010, Shimadzu, Japan, equipped with UV detector) method was described in a previous study (30). The injection volume was 20 μL and the detector wavelength was set at 345 nm. Chromatographic separation was carried out on a Phenomenex C18 column (4.6 mm × 250 mm, 5 μm) associated with a C18 pre-column (Phenomenex, USA). The mobile phase consisted of methanol-acetonitrile-water (30:30:40, *V*/*V*/*V*); isocratic elution was used. The flow rate was 0.8 ml min^{-1}. All solutions were filtered under vacuum through a 0.45-μm membrane filter and degassed ultrasonically before used.

Molecular docking studies of 3TER and xyloketal

Molecular docking was evaluated using the Surflex-Dock software (SYBYL®8.1 molecular modeling software, Tripos, USA). Crystal structure of the SOAR domain was retrieved from the RCS B Protein Data Bank (http://www.pdb.org/, PDB entry code: 3TER) (34). The molecule was sketched and minimized using Powell optimization in the presence of the Tripos force field with a convergence criterion of 0.001 kcal mol^{-1} $Å^{-1}$ and then assigned with Gasteiger-Hückel charges. Automatic docking was employed. Other parameters were established by default in the software.

Statistics

All statistics were obtained using SPSS statistics 18 software. A one-way analysis of variance (ANOVA) followed by a post hoc test was performed to evaluate the effects of different groups.

RESULTS AND DISCUSSION

Xyloketals decrease SOCE in PASMCs from C57BL/6 mice

SOCE is the main way of extracellular Ca^{2+} entry in regulating calcium signaling and cellular responses of pulmonary arterial smooth muscle cells (PASMCs). In the present

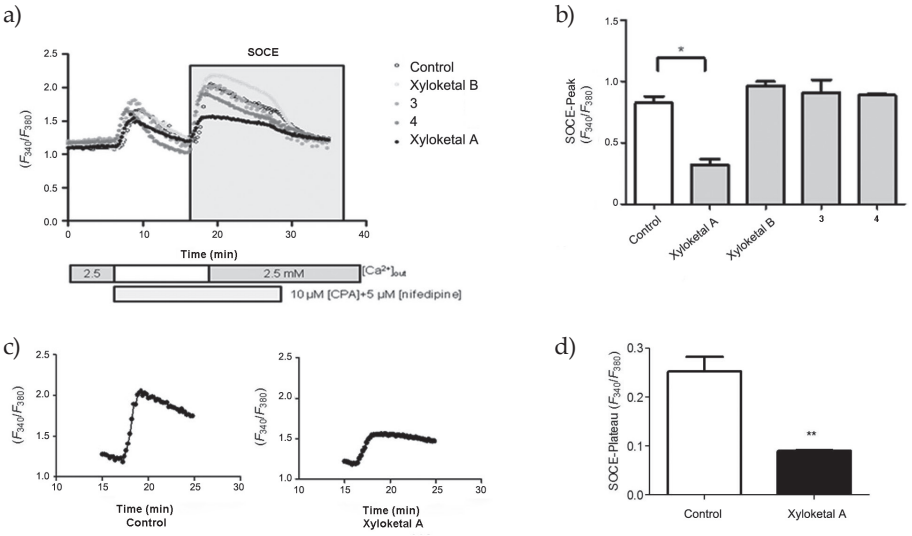

Fig. 2. Drug treatment enhances store-operated Ca^{2+} entry (SOCE) in PASMCs: a) representative trace showing changes in cytosolic Ca^{2+} concentration, b) representative records showing the amplitude of SOCE in control cells (left), and xyloketal-treated PASMCs (right), c) the peak of xyloketal A-operated Ca^{2+} entry (SOCE-peak), d) SOCE plateau phase. Data are expressed as mean ± SEM ($n = 5$). Significant difference *vs.* control: * $p < 0.05$, ** $p < 0.01$.

study, we compared the decrease of $[Ca^{2+}]_i$ due to SOCE of selected xyloketals in PASMCs isolated from C57BL/6 mice. SOCE amplitude was measured by a standard protocol (16, 19) using fura-2 dye and fluorescent microcopy in PASMCs perfused with a Ca^{2+}-free Krebs-Ringer bicarbonate solution containing 10 μmol L^{-1} cyclopiazonic acid (CPA) and 5 μmol L^{-1} nifedipine (Fig. 2a). CPA is an inhibitor of sarco (endoplasmic) reticulum Ca^{2+}-Mg^{2+}-ATPase (SERCA) and induces store depletion. Nifedipin is an inhibitor of cell membrane L-type voltage-dependent calcium channels (VDCCs) and prevents calcium entry into the cell. Five minutes following perfusion of PASMC with these two inhibitors, $[Ca^{2+}]_i$ got a transient rise, then declined to a steady state, while restoration of extracellular Ca^{2+} induced a second increase in $[Ca^{2+}]_i$ (Fig. 2a). The results showed that xyloketal A (**1**) could effectively inhibit the SOCE resulting from restoration of extracellular $[Ca^{2+}]_i$ ($p < 0.05$ compared to the control) (Fig. 2a,b). Figs. 2c,d show that $[Ca^{2+}]_i$ decreased in the SOCE peak and steady-state when xyloketal A (5 μmol L^{-1}) was applied. The same concentration of xyloketal A inhibited SOCE by > 61 % in PASMCs compared to the decrease in steady-state $[Ca^{2+}]_i$ ($p < 0.01$). The plateau phase could be markedly reduced when SOCE was blocked with xyloketal A in PASMCs. These evidences suggested that xyloketal A exerts a promising SOCE inhibition. Comparing the structures of xyloketals, the tetrahydrofuran-benzopyrane moiety in xyloketal A was highlighted as an important segment for good activity that might be a determinant factor for the inhibiting effect of SOCE. Moreover, xyloketal A, a unique ketal compound with C-3 symmetry, possesses better lipid solubility compared to other xyloketals, which makes xyloketal A a promising compound for further evaluation.

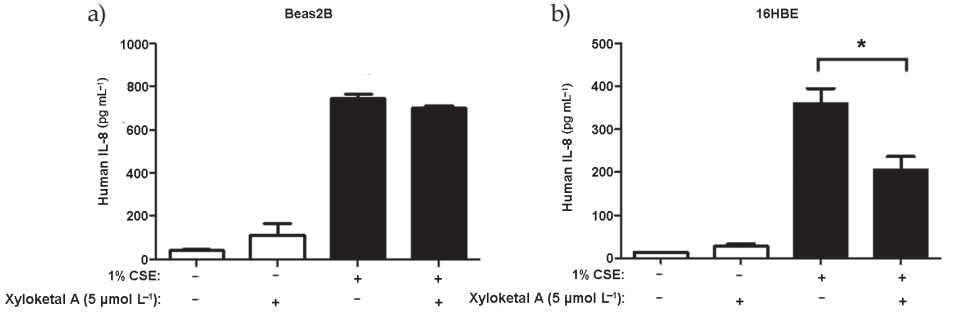

Fig. 3. Xyloketal A inhibited the IL-8 secretion from lung epithelial cells: a) Beas-2b and b) 16HBE induced by 2 % CSE. Data are expressed as mean ± SEM ($n = 5$). Significant difference *vs.* control: * $p < 0.01$.

Xyloketal A down-regulated IL-8 secretion in human lung epithelial cells

IL-8 is an important proinflammatory chemokine in airway epithelia, which contributes to the exaggerated inflammatory state of cystic fibrosis (CF) airways (31). The SOCE pathway through ORAI1 activation modulates IL-8 secretion in human airways and may contribute to the exaggerated inflammatory response in airway disease with an inflammatory component (32). Since lung inflammation has been well documented after cigarette smoke exposure, IL-8 is an important marker in early inflammation and is crucial for neutrophil recruitments common in PAH related diseases (33). As shown in Fig. 3, in our experiments xyloketal A reduced IL-8 secretion (simulated by CSE) in human epithelial cells (Beas-2b and 16HBE), indicating the anti-inflammatory effect of xyloketal A.

The parallel artificial membrane permeability assay (PAMPA)

The parallel artificial membrane permeability assay (PAMPA) is a dynamic model to study the passive diffusion of drugs through membranes and is an important assay to screen the permeability of new medicines. Using the PAMPA system, we investigated the permeability of xyloketals **1**-**4**, whereas verapamil, atenolol and ciprofloxacin were used as positive controls. The obtained results are listed in Table I. When compared to three positive controls, which moderately or hardly permeated EGG-PAMPA and HDM-PAMPA, the four examined xyloketals easily permeated EGG-PAMPA and moderately permeated HDM-PAMPA. These results implicate that the tested xyloketals easily penetrated through the cell membrane and thus might have had a certain effect on SOCE.

Molecular docking studies of 3TER and xyloketal A

Two protein molecules, stromal interaction molecule 1 (STIM1) and calcium release-activated calcium modulator 1 (ORAI1), are involved in SOCE. Since SOCE is activated through dynamic interplay between STIM1 and ORAI1 helices (18), previous studies have identified cytosolic regions within STIM1-C protein, defined as the STIM1-ORAI1-activating region (SOAR, amino acids sequence 344-442) (34). To gain the structural basis for xy-

Table I. Permeability parameters of the studied compound

Compound	log P_e	
	Egg-PAMPA	HDM-PAMPA
1	–4.93 ± 0.06 (easily)	–4.33 ± 0.08 (moderately)
2	–4.03 ± 0.08 (easily)	–3.42 ± 0.08 (easily)
3	–4.01 ± 0.12 (easily)	–3.86 ± 0.12 (easily)
4	–4.25 ± 0.005 (easily)	3.14 ± 0.03 (easily)
Verapamil	–4.96 ± 0.10 (easily)	–4.96 ± 0.18 (easily)
Atenolol	–7.14 ± 0.13 (hardly)	–6.43 ± 0.02 (hardly)
Ciprofloxacin	–5.12 ± 0.08 (moderately)	–4.64 ± 0.08 (easily)

loketal A bound to SOAR, we performed computer simulations of molecular docking between xyloketal A and the crystal structure of SOAR (3TER). As known, the residue lysine 363 (LYS363) is one of the active sites of 3TER. Our results showed that xyloketal A

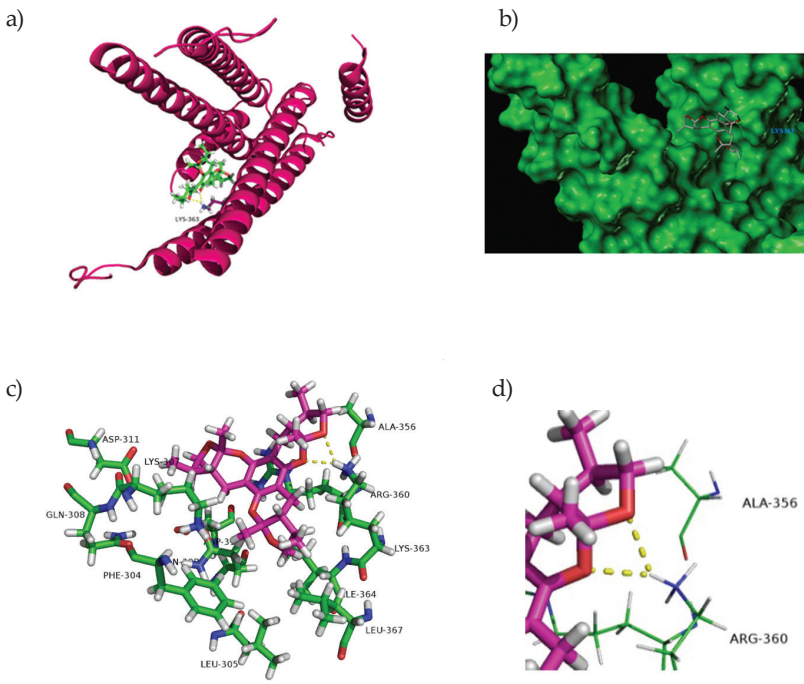

Fig. 4. Docking conformation between xyloketal A and 3TER. a) Docking model of xyloketal A together with 3TER, b) docking conformation between xyloketal A and 3TER in the Connolly mode, c) molecular docking model of xyloketal A inside an active site (5 Å) of 3TER, d) the key binding bonds of xyloketal A with the amino-acid residues of 3TER.

could bind with this residue in the pocket and may generate non-covalent interaction with the oxygen atom of the tetrahydrofuran-benzopyrane moiety (Fig. 4), and that the distance between this active residues and xyloketal A was about 5 Å.

CONCLUSIONS

Xyloketals have been reported to be protective agents against a variety of pathophysiological stimuli. Their unusual molecular structures possess calcium channel blocking activities. Store-operated calcium entry (SOCE) plays an important role in the development of chronic hypoxic pulmonary hypertension. We have proven that xyloketal A, a unique compound with C-3 symmetry, is a SOCE blocker. At the same time, a parallel artificial membrane permeability assay (PAMPA) experiment has proven that it is easily transported through the cell membrane. Our results suggest that xyloketal A might be a new candidate for the treatment of PAH.

Acknowledgements. – This work was supported by the National Natural Science Foundation of China (21172271) and the Natural Science Foundation of Guangdong Province, China (Grant No. S2011020001231).

REFERENCES

1. S. E. Peel, B. Liu and I. P. Hall, Orai and store-operated calcium influx in human airway smooth muscle cells, *Am. J. Respir. Cell Molec. Biol.* **38** (2008) 744–749; https://doi.org/10.1165/rcmb.2007-0395OC
2. H. Mogami, K. Nakano, A. V. Tepikin and O. H. Petersen, Ca^{2+} flow via tunnels in polarized cells: recharging of apical Ca^{2+} stores by focal Ca^{2+} entry through basal membrane patch, *Cell* **88** (1997) 49–55; https://doi.org/10.1016/S0092-8674(00)81857-7
3. I. F. Abdullaev, J. M. Bisaillon, M. Potier, J. C. Gonzalez, R. K. Motiani and M. Trebak, Stim1 and orai1 mediate CRAC currents and store-operated calcium entry important for endothelial cell proliferation, *Circ. Res.* **103** (2008) 1289–1299; https://doi.org/10.1161/01.RES.0000338496.95579.56
4. C. V. Remillard and J. X. J. Yuan, TRP channels, CCE, and the pulmonary vascular smooth muscle, *Microcirculation* **13** (2006) 671–692; https://doi.org/10.1080/10739680600930313
5. M. Potier, J. C. Gonzalez, R. K. Motiani, I. F. Abdullaev, J. M. Bisaillon, H. A. Singer and M. Trebak, Evidence for STIM1- and Orai1-dependent store operated calcium influx through ICRAC in vascular smooth muscle cells: role in proliferation and migration, *FASEB J.* **23** (2009) 2425–2437; https://doi.org/10.1096/fj.09-131128
6. F. R. Giachini, C. W. Chiao, F. S. Carneiro, V. V. Lima, Z. N. Carneiro, A. M. Dorrance, R. C. Tostes and R. C. Webb, Increased activation of stromal interaction molecule-1/Orai-1 in aorta from hypertensive rats: a novel insight into vascular dysfunction, *Hypertension* **53** (2009) 409–416; https://doi.org/10.1161/HYPERTENSIONAHA.108.124404
7. R. W. Guo, H. Wang, P. Gao, M. Q. Li, C. Y. Zeng, Y. Yu, J. F. Chen, M. B. Song, Y. K. Shi and L. Huang, An essential role for stromal interaction molecule 1 in neointima formation following arterial injury, *Cardiovasc. Res.* **81** (2009) 660–668; https://doi.org/10.1093/cvr/cvn338
8. A. Braun, D. Varga-Szabo, C. Kleinschnitz, I. Pleines, M. Bender, M. Austinat, M. Bösl, G. Stoll and B. Nieswandt, Orai1 (CRACM1) is the platelet SOC channel and essential for pathological thrombus formation, *Blood* **113** (2009) 2056–2063; https://doi.org/10.1182/blood-2008-07-171611
9. A. Berna-Erro, A. Braun, R. Kraft, C. Kleinschnitz, M. K. Schuhmann, D. Stegner, T. Wultsch, J. Eilers, S. G. Meuth, G. Stoll and B. Nieswandt, STIM2 regulates capacitive Ca^{2+} entry in neurons and plays a key role in hypoxic neuronal cell death, *Sci. Signal.* **2** (2009) ra67; https://doi.org/10.1126/scisignal.2000522

10. H. Zbidi, J. J. López, N. B. Amor, A. Bartegi, G. M. Salido and J. A. Rosado, Enhanced expression of STIM1/Orai1 and TRPC3 in platelets from patients with type 2 diabetes mellitus, *Blood Cells Mol. Dis.* **43** (2009) 211–213; https://doi.org/10.1016/j.bcmd.2009.04.005
11. M. Zhu, L. Chen, P. Zhao, H. Zhou, C. Zhang, S. Yu, Y. Lin and X. Yang, Store-operated Ca^{2+} entry regulates glioma cell migration and invasion via modulation of Pyk2 phosphorylation, *J. Exp. Clin. Cancer Res.* **33** (2014) 98–98; https://doi.org/10.1186/s13046-014-0098-1
12. M. Umemura, E. Baljinnyam, S. Feske, M. S. De Lorenzo, L.-H. Xie, X. Feng, K. Oda, A. Makino, T. Fujita, U. Yokoyama, M. Iwatsubo, S. Chen, J. S. Goydos, Y. Ishikawa and K. Iwatsubo, Store-operated Ca^{2+} entry (SOCE) regulates melanoma proliferation and cell migration, *PLoS One* **9** (2014) e89292; https://doi.org/10.1371/journal.pone.0089292
13. J. Zhang, J. Wei, M. Kanada, L. Yan, Z. Zhang, H. Watanabe and S. Terakawa, Inhibition of store-operated Ca^{2+} entry suppresses EGF-induced migration and eliminates extravasation from vasculature in nasopharyngeal carcinoma cell, *Cancer Lett.* **336** (2013) 390–397; https://doi.org/10.1016/j.canlet.2013.03.026
14. C. Holzmann, T. Kilch, S. Kappel, A. Armbrüster, V. Jung, M. Stöckle, I. Bogeski, E. C. Schwarz and C. Peinelt, ICRAC controls the rapid androgen response in human primary prostate epithelial cells and is altered in prostate cancer, *Oncotarget*. **4** (2013) 2096–2107; https://doi.org/10.18632/oncotarget.1483
15. J. Wang, Q. Jiang, L. Wan, K. Yang, Y. Zhang, Y. Chen, E. Wang, N. Lai, L. Zhao, H. Jiang, Y. Sun, N. Zhong, P. Ran and W. Lu, Sodium tanshinone IIa sulfonate inhibits canonical transient receptor potential expression in pulmonary arterial smooth muscle from pulmonary hypertensive rats, *Proc. Natl. Acad. Sci. USA* **48** (2013) 125–134; https://doi.org/10.1165/rcmb.2012-0071OC
16. S. Feske, ORAI1 and STIM1 deficiency in human and mice: roles of store-operated Ca^{2+} entry in the immune system and beyond, *Immunol. Rev.* **231** (2009) 189–209; https://doi.org/10.1111/j.1600-065X.2009.00818.x
17. K. Ohga, R. Takezawa, T. Yoshino, T. Yamada , Y. Shimizu and J. Ishikawa, The suppressive effects of YM-58483/BTP-2, a store-operated Ca^{2+} entry blocker, on inflammatory mediator release in vitro and airway responses in vivo, *Pulm. Pharmacol. Ther.* **21** (2008) 360–369; https://doi.org/10.1016/j.pupt.2007.09.003
18. P. B. Stathopulos, R. Schindl, M. Fahrner, L. Zheng, G. M. Gasmi-Seabrook, S. Gasmi, M. Muik, C. Romanin and M. Ikura, STIM1/Orai1 coiled-coil interplay in the regulation of store-operated calcium entry, *Nat. Commun.* **12** (2013) 1–12; https://doi.org/10.1038/ncomms3963
19. Y. Lin, X. Wu, S. Feng, G. Jiang, J. Luo, S. Zhou, L. L. P. Vrijmoed, E. B. G. Jones, K. Krohn, K. Steingröver and F. Zsila, Five unique compounds: Xyloketals from mangrove fungus *Xylaria* sp. from the South China sea coast, *J. Org. Chem.* **66** (2001) 6252–6256; https://doi.org/10.1021/jo015522r
20. X. Y. Wu, X. H. Liu, Y. C. Lin, J. H. Luo, Z. G. She, H. J. Li, W. L. Chan, S. Antus, T. Kurtan, B. Elsässer and K. Krohn, Xyloketal F: A strong L-calcium channel blocker from the mangrove fungus *Xylaria* sp. (#2508) from the South China sea coast, *Eur. J. Org. Chem.* **2005** (2005) 4061–4064; https://doi.org/10.1002/ejoc.200500326
21. Z. Xu, B. Lu, Q. Xiang, Y. Li, S. Li, Y. Lin and J. Pang, Radical-scavenging activities of marine-derived xyloketals and related chromanes, *Acta Pharm. Sinca B* **3** (2013) 322–327; https://doi.org/10.1016/j.apsb.2013.06.008
22. W. L. Chen, Y. Qian, W. F. Meng, J. Y. Pang, Y. C. Lin and Y. Y. Guan, A novel marine compound xyloketal B protects against oxidized LDL-induced cell injury in vitro, *Biochem. Pharmacol.* **78** (2009) 941–950; https://doi.org/10.1016/j.bcp.2009.05.029
23. Z. Xu, Y. Li, Q. Xiang, Z. Pei, X. Liu, B. Lu, L. Chen, G. Wang, J. Pang and Y. Lin, Design and synthesis of novel xyloketal derivatives and their vasorelaxing activities in rat thoracic aorta and angiogenic activities in zebrafish angiogenesis screen, *J. Med. Chem.* **53** (2010) 4642–4653; https://doi.org/10.1021/jm1001502

24. M. Romero, I. Sanchez and M. D. Pujol, New advances in the field of calcium channel antagonists: cardiovascular effects and structure-activity relationships, *Curr. Med. Chem.* **1** (2003) 113–141; https://doi.org/10.2174/1568016033477487
25. G. B. Waypa, S. W. Osborne, J. D. Marks, S. K. Berkelhamer, J. Kondapalli and P. T. Schumacker, Sirtuin 3 deficiency does not augment hypoxia-induced pulmonary hypertension, *Amer. J. Respir. Cell Molec. Biol.* **49** (2013) 885–891; https://doi.org/10.1165/rcmb.2013-0191OC
26. B. Manoury, C. Lamalle, R. Oliveira, J. Reid and A. M. Gurney, Contractile and electrophysiological properties of pulmonary artery smooth muscle are not altered in TASK-1 knockout mice, *J. Physiol.* **589** (2011) 3231–3246; https://doi.org/10.1113/jphysiol.2011.206748
27. A. Ogawa, A. L. Firth, W. Yao, M. M. Madani, K. M. Kerr, W. R. Auger, S. W. Jamieson, P. A. Thistlethwaite and J. X. J. Yuan, Inhibition of mTOR attenuates store-operated Ca^{2+} entry in cells from endarterectomized tissues of patients with chronic thromboembolic pulmonary hypertension, *Amer. J. Physiol. Lung Cell. Mol. Physiol.* **297** (2009) L666–676; https://doi.org/10.1152/ajplung.90548.2008
28. K. Yang, W. Lu, Q. Jiang, X. Yun, M. Zhao, H. Jiang and J. Wang, Peroxisome proliferator-activated receptor γ-mediated inhibition on hypoxia-triggered store-operated calcium entry. A caveolin-1-dependent mechanism, *Am. J. Respir. Cell Molec. Biol.* **53** (2015) 882–892; https://doi.org/10.1165/rcmb.2015-0002OC
29. K. V. Sandhya, G. S. Devi and S. T. Mathew, Liposomal formulations of serratiopeptidase: In vitro studies using PAMPA and Caco-2 models, *Mol. Pharm.* **5** (2008) 92–97; https://doi.org/10.1021/mp700090r
30. W. Zhang, Y. Liu, H. Yang, Z. Li, Y. Huang, Z. Xu, Y. Lin, Q. Xiang and J. Pang, A validated high-performance liquid chromatographic method with diode-array detection for the estimation of xyloketal B in rat plasma, *J. Chromatogr. B Analyt. Technol. Bio. Life Sci.* **855–856** (2012) 24–29; https://doi.org/10.1016/j.jchroma.2011.12.005
31. M. Bédard, C. D. McClure, N. L. Schiller, C. Francoeur, A. Cantin and M. Denis, Release of interleukin-8, interleukin-6, and colony-stimulating factors by upper airway epithelial cells: implications for cystic fibrosis, *Am. J. Respir. Cell Mol. Biol.* **9** (1993) 455–462; https://doi.org/10.1165/ajrcmb/9.4.455
32. H. Balghi, R. Robert, B. Rappaz, X. Zhang, A. Wohlhuter-Haddad, A. Evagelidis, Y. Luo, J. Goepp, P. Ferraro, P. Roméo, M. Trebak, P. W. Wiseman, D. Y. Thomas and J. W. Hanrahan, Enhanced Ca^{2+} entry due to Orai1 plasma membrane insertion increases IL-8 secretion by cystic fibrosis airways, *FASEB J.* **25** (2011) 4274–4291; https://doi.org/10.1096/fj.11-187682
33. G. W. Hunninghake and R. G. Crystal, Cigarette smoking and lung destruction: Accumulation of neutrophils in the lungs of cigarette smokers, *Am. Rev. Respir. Dis.* **128** (1983) 833–838; https://doi.org/10.1164/arrd.1983.128.5.833
34. X. Yang, H. Jin, X. Cai, S. Li and Y. Shen, Structural and mechanistic insights into the activation of stromal interaction molecule 1 (STIM1), *Proc. Natl. Acad. Sci. USA* **109** (2012) 5657–5662; https://doi.org/10.1073/pnas.1118947109